Method for Modeling Post-mortem Biometric 3-D Fingerprints

Srijith Rajeev, Shreyas Kamath K. M, Sos S. Agaian
Department of Electrical and Computer Engineering, The University of Texas at San Antonio,
One UTSA Circle, San Antonio, TX 78249

ABSTRACT

Despite the advancements of fingerprint recognition in 2-D and 3-D domain, authenticating deformed/post-mortem fingerprints continue to be an important challenge. Prior cleansing and reconditioning of the deceased finger is required before acquisition of the fingerprint. The victim's finger needs to be precisely and carefully operated by a medium to record the fingerprint impression. This process may damage the structure of the finger, which subsequently leads to higher false rejection rates. This paper proposes a non-invasive method to perform 3-D deformed/post-mortem finger modeling, which produces a 2-D rolled equivalent fingerprint for automated verification. The presented novel modeling method involves masking, filtering, and unrolling. Computer simulations were conducted on finger models with different depth variations obtained from Flashscan3D LLC. Results illustrate that the modeling scheme provides a viable 2-D fingerprint of deformed models for automated verification. The quality and adaptability of the obtained unrolled 2-D fingerprints were analyzed using NIST fingerprint software. Eventually, the presented method could be extended to other biometric traits such as palm, foot, tongue etc. for security and administrative applications.

Keywords: biometric, fingerprint, 3-D, unrolling, modeling, post-mortem, deformed, non-parametric, verification

1. INTRODUCTION

The biometric method of authenticating an individual came into emergence in the 20th century and has been used extensively [1]. Fingerprint verification is preferred over other biometric methods including retina, DNA, and facial patterns due to its distinctiveness and ease of acquisition [2]. Fingerprints are obtained by pressing or rolling an inked finger against a platen [3] surface; in addition, a digital image is produced using a general purpose scanner [4, 5]. Developments in the field led to utilization of contact based fingerprint image acquisition sensors such as optical, capacitive, solid-state, thermal, ultrasound, etc. [3, 6, 7], which directly produces a fingerprint image by sensing the finger surfaces[4]. Currently, fingerprint verification plays a major role in the field of forensics, security and commercial application such as US-VISIT's IDENT program, the FBI's NGI (formerly IAFIS) service [8], passports, civilian identification cards, access control, bio-cryptography etc. [9-12].

Fingerprints contain unique minutiae features such as ridges, bifurcations, valleys, islands etc. [8, 13, 14]. In a touch-based two dimensional (2-D) fingerprint system, the finger needs to be physically held on the sensor surface for acquisition. This process needs a trained professional. As a result, a slight shift during capture process may cause the fingerprint features to be distorted [3, 5]. During acquisition, a curved human finger is flattened on a 2-D plane, thus shifting the features from its actual position [15]. The quality of the fingerprint image is also dependent on individual artifacts such as skin conditions as well as deformations, pressure applied etc. [16]. Also, geometrical distortions of the features may be introduced because of these non-ideal conditions [17]. Hygiene is a major concern in touch-based systems because of repetitive usage. This can lead to deposition of sweat, dust, and grease on the sensor [18].

An approach to overcome these shortcomings was to replace the touch-based 2-D system with a non-invasive three-dimensional (3-D) fingerprint scanner. A 3-D scanner can capture texture of the surface along with depth information, thus providing detailed information about the features of the finger. Some of the advantages of 3-D scanners are:

- Production of better image quality, resulting in the improvement of matching rates [12, 19-21].
- Distortion-free images are achieved as dry skin, sweat, oil, etc. do not affect a touchless interface [19, 20]
- Partial/-scarred fingerprints can be captured more efficiently [19]
- Other geometric constraints can be determined such as volume, detailed ridge information, thickness etc.

**This project was partially supported by Award No. 2014-IJ-CX-K003, awarded by the National Institute of Justice, Office of Justice Programs, U.S. Department of Justice. The opinions, findings, and conclusions or recommendations expressed in this paper are those of the authors and do not necessarily reflect those of the Department of Justice.

Mobile Multimedia/Image Processing, Security, and Applications 2016, edited by Sos S. Agaian, Sabah A. Jassim, Proc. of SPIE Vol. 9869, 98690S · © 2016 SPIE
CCC code: 0277-786X/16/$18 · doi: 10.1117/12.2224386

3-D fingerprint acquisition is performed using popular methods such as stereo vision [17], structured light scanning [22] and multiple camera view reconstruction [19]. However, once 3-D models are obtained, problems arise in the domain of matching; this is because agencies around the world use a 2-D fingerprint database. Acquiring 3-D databases and necessary software for verification is not only expensive but also time consuming. Furthermore, 3-D fingerprint models cannot be directly matched with 2-D fingerprint databases. Chen *et al.* proposed that an interim solution is to unroll the 3-D models to an equivalent 2-D fingerprint image and then match them with the existing 2-D databases[23]. In order to virtually unwrap 3-D finger models, several unrolling algorithms have been proposed [24]. They can be divided into two categories i.e. parametric and non-parametric unrolling algorithms [4, 23]. Parametric unrolling method deals with the assumption that the finger surface can be represented as a tube [4, 22, 25], cylinder [4, 23] or sphere [4, 21] which are also known as parametric surfaces. The non-parametric unrolling methods consider the Euclidean distance between two successive points in the 3-D mesh, mainly aiming at geodesic preservation, but does not consider the shape of the model [23]. Although touchless 3-D fingerprint technology has many advantages, the system is neoteric, and hence contains few drawbacks like non-uniform image resolution, low contrast between valleys and ridges, and a sensitive scanner.

A major concern in the forensic and criminal justice communities is the identification of the deceased. Fingerprint recognition is a preferred method in which post-mortem (PM) fingerprints are compared with ante-mortem (AM) fingerprints to confirm the identification of an individual [26, 27]. However, the process of obtaining forensic-quality PM fingerprint records is an arduous task. Prior to acquisition, the PM finger may require reconditioning techniques depending on the amount of decomposition and loss of fluids [27, 28]. The decedent's finger needs to be carefully and precisely manipulated by a medium to record the fingerprint impression [26]. Furthermore, a touch-based acquisition system increases the chances of degradation of the PM friction ridge detail. As such, a 3-D touchless system might provide a suitable solution to overcome the problem of acquisition and verification of deformed/PM fingerprints. Lastly, existing unrolling and 3-D identification methods do not consider the presence of deformities in the finger.

This paper presents an algorithm to unroll 3-D deformed/PM fingerprints for the first time, which can be used for automated verification. The 3-D model of the finger is pre-processed to remove noise, and then a compensation model is created to predict and compensate deformities in the finger. Finally, the 3-D finger is modeled to a flat plane in order to obtain a 2-D equivalent fingerprint. The rest of this paper is organized as follows: descriptions of related systems are presented in Section 2, the proposed system is described in Section 3, and computer simulations and performances are given in Section 4. Finally, conclusions and future works are drawn in Section 5.

2. RELATED WORK

Unrolling algorithms can be broadly classified into, parametric method, wherein the 3-D model to be unrolled is represented by a known geometrical model, and non-parametric method, wherein no assumption to the shape of the model is made. Some of the implementations of both these methods are described in this section.

Abramovich et al. show a parametric method that unrolls the 3-D model into a 2-D image by circular approximation of the cross sections of the finger [25]. Each cross section in resulting image has a unique center and radius. The location of the projection can be determined by its corresponding unrolled pixel. However, this process is designed for slap fingerprint images only.

Wang et al. unrolled 3-D fingerprints using the fit sphere unwrapping algorithm [22], assuming (X^c, Y^c, Z^c) are the center of the sphere, R is the radius, (X_k, Y_k, Z_k) are the points on the 3-D model, then the distance between the point on the 3-D model and sphere is determined using equation (1). The unrolling procedure is forced to begin from the center of the model by adjusting the coordinates using equations (2), (3), and (4). This results in the North Pole protruding from the center of the 3-D model. Next, the spherical coordinates of the point cloud are obtained, and using linear unwrapping maps, the distance between consecutive vertical points, and consecutive horizontal points are calculated. Finally, the distortions that occur during unwrapping are corrected and the image is scaled.

$$D = [(X_k - X^c)^2 + (Y_k - Y^c)^2 + (Z_k - Z^c)^2]^{1/2} - R \quad (1)$$

$$X_k = X_k - X^c - \frac{\sum_{g=1}^{g=K}(X_k - X^c)}{K} \quad (2)$$

$$Y_k = Y_k - Y^c - \frac{\sum_{g=1}^{g=K}(Y_k - Y^c)}{K} \quad (3)$$

$$Z_k = Z_k - Z^c \quad (4)$$

A parametric method described in [23] projects a 3-D finger model on a 3-D cylindrical model and then unrolls the cylinder to obtain a 2-D fingerprint. The algorithm assumes that the finger model consists of cross sections of circles with equal radius. Let P be a point on the model, which can be represented by its 3-D coordinates shown in equation (5). This point is projected onto the cylinder of known dimensions using equations (6) and (7).

$$P_{3D} = (X, Y, Z) \quad (5)$$

where, X,Y,Z are the 3-D coordinates

$$\theta = \tan^{-1}\left(\frac{X}{Y}\right) \quad (6)$$

$$P_{2D} = (\theta, Z) \quad (7)$$

In [22], Wang et al. presented an unrolling algorithm that unfolds an elastic tube, geometrically fit to the peaks and valleys of the 3-D finger. They used multiple rings of varying radii along the height of the finger model, and a moving average filter, for smoothing the surface. The model is then unrolled with controlled pixels per inch (PPI) values to reduce distortion. This image is fused with an unrolled albedo image to improve the quality.

Chen et al. presents a non-parametric method that proposes to up-sample the model and divide it into thin slices [23]. Unrolling is performed on each slice individually, thus minimizing the stretching effect. Zhao et al. presents a method to simulate pressure on the 3-D model while unrolling which increases compatibility between 2-D fingerprint images and unrolled images [21]. They also describe an approach to unroll 3-D finger models based on the adaptive sampling intervals by dividing the 3-D model into a set of thin slices.

Fatehpuria et al. discuss yet another non-parametric method and propose a method to extract the surface of the 3-D finger model [29]. Using a weighted, non-linear, least square algorithm, the surface is smoothened. This extracted surface is unrolled using the 'Springs algorithm' [30]. The 3-D point cloud is assumed to be a cluster of inter-connected points with mass. These points are assumed to be connected using springs. Let e_i be the individual energy of the spring, d_i be the Euclidean distance between the points connected by the i^{th} spring, and r_i be the relaxed length, then the energy in a spring is calculated using equation (8). The total energy (e) of a point, i.e. the summation of all the springs connected to the points is given by equation (9)

$$e_i = \text{sign}(d_i - r_i).(d_i - r_i)^2 \quad (8)$$

$$e = \sum_{i=1}^{n} e_i \quad (9)$$

The general algorithm is to compress those springs whose relaxed length is greater than the current length and vice-versa. This process moves the points to and from such that they reach a balanced state with minimum energy. This algorithm is iteratively implemented to get the unrolled fingerprint. The unrolled surface will be smooth and thus, to gain texture in the final unrolled image, the difference between the smoothed model and the original model is added.

Shafaei et al. use the same approach as Fatehpuria et al. [29] to unroll the 3-D model and then use curvature analysis to apply the fingerprint texture on the smooth unrolled surface [20] . The finger texture is extracted using a Gaussian filter. The ridges and valleys are identified using curvature analysis and colored black if they are ridges and white if the points are valleys.

3. PROPOSED UNROLLING ALGORITHM FOR POST-MORTEM FINGER MODELS

This section discusses the proposed unrolling algorithm. This process is performed to model/unroll the captured deformed fingerprint for verification. The steps involved are shown below:

Algorithm for unrolling deformed 3-D model

1.	Input the deformed 3-D fingerprint mesh structure
2.	Perform masking and use filters to remove noise if present
3.	Extract the ridge information
4.	Unroll the deformed 3-D finger
5.	Apply the ridge information
6.	Output the unrolled 3-D model

3.1 Deformed 3-D model initialization

Deformed 3-D models were provided by Flashscan3D [31]. These models were deformed manually to three different levels. Figure 1 shows the original or non-deformed model. Figure 2 displays a model with the least deformations. Figure 3 shows another model, which has greater deformations, and figure 4 shows the model with the highest amount of deformation in the database. The models were chosen to test the robustness of the algorithm in unrolling models of varying deformities.

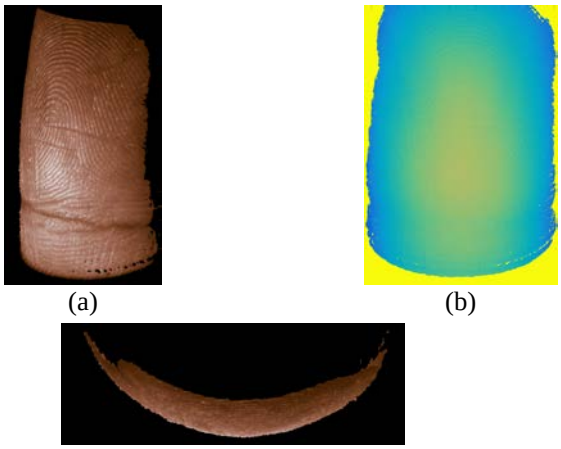

(a) (b)

(c)

Figure 1: (a) shows the original model, (b) shows the depth map, and (c) shows the top view

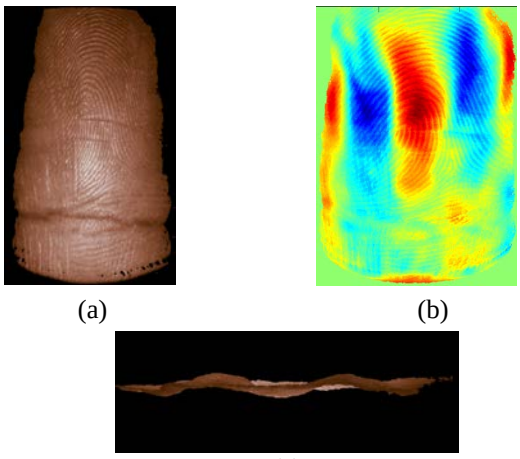

(a) (b)

(c)

Figure 2: (a) shows the model, (b) shows the depth map, and (c) shows the top view

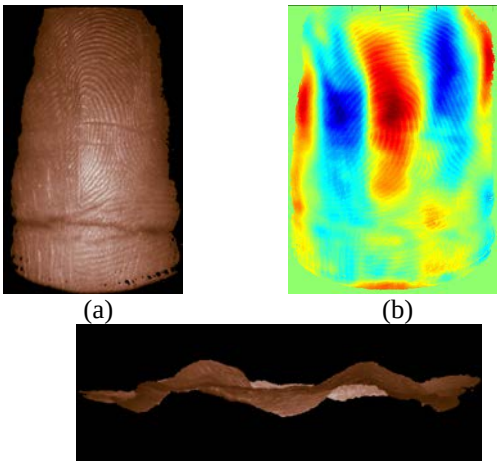

Figure 3: (a) shows the model, (b) shows the depth map, and (c) shows the top view

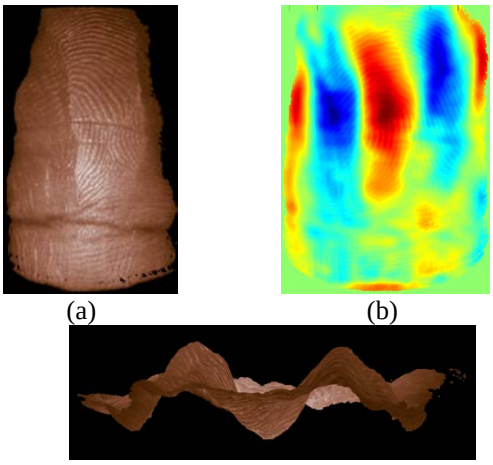

Figure 4: (a) shows the model, (b) shows the depth map, and (c) shows the top view

Example (b) in figures (1-4) shows the depth of the models. Example (c) in figures (1-4) displays the degree of deformation. Colors indicate the relative position of the points in the model. Assuming the model is placed at (0, 0, 0), the points in red indicate that they have relatively greater positive depth compared to the points in blue; higher the intensity of the point, higher the magnitude. The models are in the MAT5 format [32], i.e. there exists five files associated with each model, texture image, intensity image, and the X, Y, Z coordinate files. This format is used because it is unsophisticated and extremely flexible.

3.2 Pre-processing – masking and extracting fingerprint ridge information

The quality of the 3-D model is dependent on many notable factors: lighting, camera, reconstruction algorithm etc. Consequently, a pre-processing procedure is necessary to ensure that the unrolled 3-D model can be utilized for fingerprint verification purposes. Masking is performed by identifying the region of interest (ROI) and removing the points outside the ROI. The results of filtering the noise are shown in Figure 5 (a) and (b).

Another approach to removing points within the boundaries is to perform block wise standard deviation filtering. After eliminating the noise, the fingerprint texture needs to be preserved, as it contains vital minutiae features. If the textured model is unrolled, the ridges and valleys will get modeled as well. Therefore, the texture is extracted and smoothened using a Gaussian 2-D filter. Figure 5 (c) shows the extracted texture.

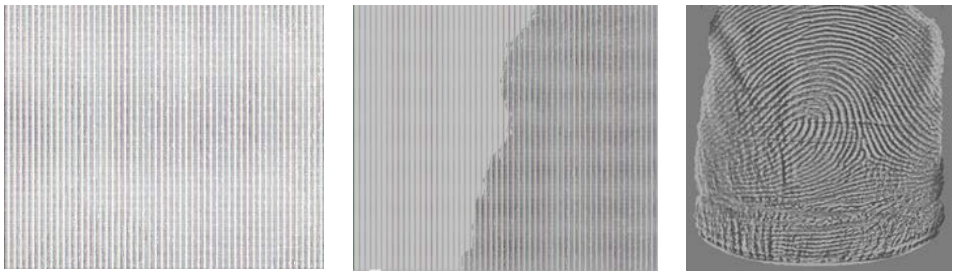

(a) (b) (c)

Figure 5: (a) shows the cross section of the points with noise, (b) shows the same cross section after masking, and (c) shows the extracted fingerprint information.

3.3 Unroll smooth deformed finger model

Parametric unrolling methods make an assumption of the shape of the 3-D model, and hence, applying it on deformed models will result in erroneous results. A non-parametric approach is more suitable for this application. This subsection summarizes the deformed unrolling procedure.

Post-mortem fingerprints are unpredictable in both quality as well as continuity, and are vastly different from ante-mortem fingerprints. Dis-continuities need to be identified and a compensation measure has to be developed to ensure the algorithm is robust. The central area of a human finger provides most of the information and therefore, the process of unrolling is instigated from the center and then moved to the sides. The basic setup of the compensation model is to identify holes in the model and determine the coordinates of the points along the hole. Let $P(x, y, z)_{i,j}$ be a point in the model, and x, y, and z be the surface, height, and depth of the point, and i, j be the indices used to identify the point. Then a simple compensation model can be created using equation (10).

$$\text{If } P(x,y,z)_{i,j} == \text{NaN}$$
$$\text{Then, } \hat{P}(\hat{x},\hat{y},\hat{z})_{i,j} = P(x,y,z)_{i-1,j-1} \quad (10)$$
$$\text{where, } \hat{P} \text{ is the point in the compensation model}$$

For non-forensic purposes, interpolation can be performed to fill holes. But, this would create redundant information which would eventually deter a forensic investigation. The compensation model is a temporary/transient model and it does not affect the unrolling procedure. It will facilitate in avoiding the holes in the model during the unrolling process. Next, the Euclidean distance between points and its corresponding location is calculated, using equations (11) and (12) if a hole is encountered. Otherwise, equations (13) and (14) can be used for normal circumstances.

$$\hat{T} = \sqrt{\left(\hat{x}(i,j) - x(i,j+1)\right)^2 + \left(\hat{z}(i,j) - z(i,j+1)\right)^2} \quad (11)$$

$$S(i,j+1) = \bar{S}(i,j) \pm \hat{T} \quad (12)$$

$$T = \sqrt{\left(x(i,j) - x(i,j+1)\right)^2 + \left(z(i,j) - z(i,j+1)\right)^2} \quad (13)$$

$$S(i,j+1) = S(i,j) \pm T \quad (14)$$

$\hat{T}$ calculates the Euclidean distance using information from the compensation model. S is the unrolled coordinate and $\bar{S}$ is the last valid unrolled coordinate before encountering the hole in the 3-D deformed model. Once the algorithm is run on all the points from the center till the edges, a raw unrolled 3-D model is obtained. The original texture extracted in section 3.2 is added to its corresponding point in the unrolled model to provide the vital minutiae features. Masking can be further performed to remove stray points.

4. COMPUTER SIMULATIONS

Figure 6 (b-d) show the results of the proposed unrolling method. Figure 6(a) is the 2-D equivalent unrolled image of the same model without any deformations. Visually figure 6(b) and 6(c) look similar to figure 7(a), but figure 6(d) is spatially distorted. However, the quality of the ridge is maintained throughout the transformation. The unrolled fingerprint images are subjected to a wide variety of distortions and changes during capture, pre-processing, and modeling. These procedures may degrade the visual quality of the image [33]. The unrolled images are evaluated for error measurements against the unrolled image of non-deformed model (original model) using algorithms such as EME [34], AME [35], and a modified SDME[36] which follows the equation 15. Table 1 shows the image error measurements. Based on the scores, it can be inferred that the unrolled deformed images are similar to the original 2-D equivalent fingerprint.

$$\mathrm{SDME} = -\frac{1}{k_1 k_2}\sum_{l=1}^{k_1}\sum_{l=1}^{k_2} 20\ln\left|\frac{I_{\mathrm{max,diagonals}} - 2I_{\mathrm{center,k,l}} + I_{\mathrm{min,diagonals}}}{I_{\mathrm{max,diagonals}} + 2I_{\mathrm{center,k,l}} + I_{\mathrm{min,diagonals}}}\right| \tag{15}$$

where an image is divided into k_1 x k_2 blocks, $I_{\mathrm{max,diagonals}}$ and $I_{\mathrm{min,diagonals}}$ are the maximum and minimum values of the pixels along the diagonals in each block separately, and $I_{\mathrm{center,k,l}}$ is the intensity of the center pixel in each block.

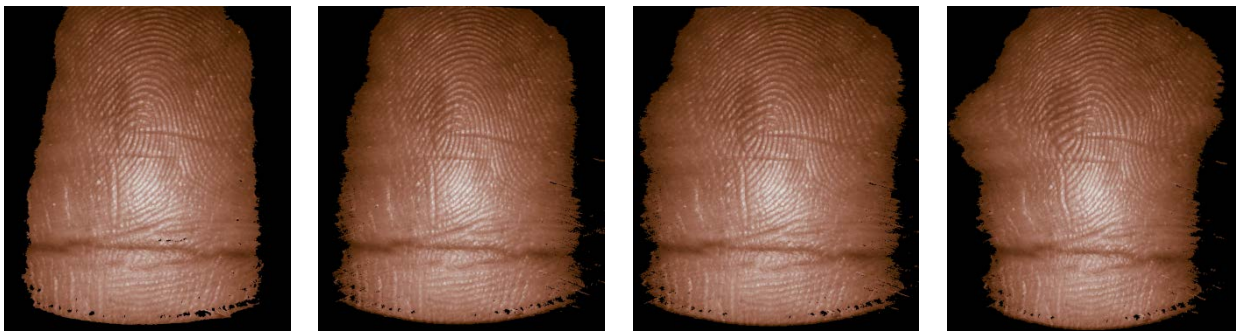

(a) (b) (c) (d)

Figure 6: (a) shows the 2-D equivalent unrolled image of the normal or non-deformed 3-D finger, and (b-d) shows the 2-D equivalent unrolled images of deformed 3-D finger models.

Table 1. Image error measurements of unrolled images

Method	Original	Model 1	Model 2	Model 3	Average Image error measure (All unrolled images)
Modified SDME (5x5 blocks)	35.78	35.60	35.65	35.90	35.7325
Modified SDME (3x3 blocks)	40.78	40.26	40.45	40.69	40.545
EME	2.14	2.14	2.19	1.82	2.0725
AME	20.79	20.79	20.94	21.15	20.9175

The unrolled images are further enhanced, filtered and binarized to provide fingerprint images as shown in figure 7 (a-d). The variations in visual quality of the binarized images were measured using EME [34], modified SDME [36], and AME [35], and the results are tabulated below. The binarized images were then run through NIST's MINDTCT [37] to detect the total number of minutiae. The detected minutiae are shown in figure 8. The results show that more minutiae were detected in the unrolled fingerprint images of the deformed models. However, few of the minutiae are significantly displaced from their original position.

(a) (b) (c) (d)

Figure 7 (a) shows enhanced, binarized output of the normal unrolled image, and (b-d) shows enhanced, binarized output of the unrolled deformed finger models.

Table 2. Image error measurements of binarized images

Method	Original	Model 1	Model 2	Model 3	Average Image error measure (All unrolled binarized images)
Modified SDME (5x5 blocks)	8.86	8.56	8.65	8.63	8.675
Modified SDME (3x3 blocks)	15.34	14.86	14.90	14.88	14.995
EME	27.84	28.13	29.68	28.01	28.415
AME	2.67	2.48	2.46	2.50	2.5275

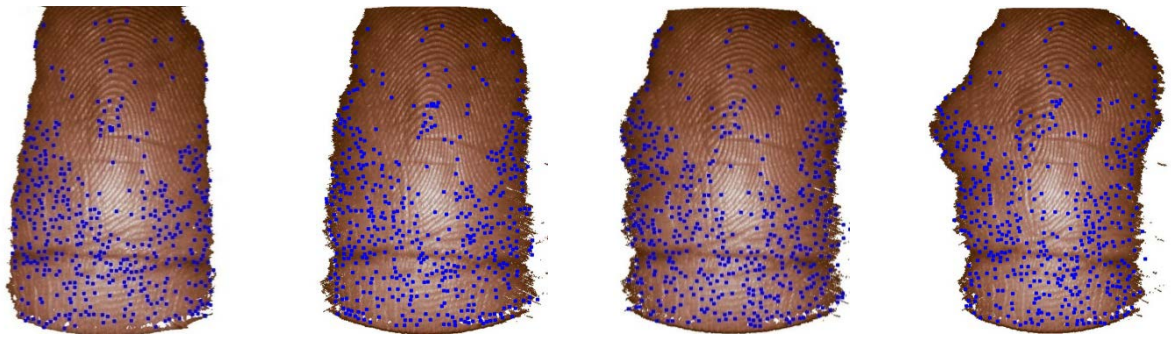

NIST Minutiae detected: 424 (a) | NIST Minutiae detected: 484 (b) | NIST Minutiae detected: 507 (c) | NIST Minutiae detected: 473 (d)

Figure 8: (a) shows the detected minutiae on the unrolled images of the original, and (b-d) shows the minutiae on unrolled images of the deformed models.

It can be noticed from the unrolling algorithm and its simulation that the effect of pressure on the finger during slap or rolling acquisition is not taken into consideration. This distortion can reduce the accuracy during fingerprint verification.

5. CONCLUSION AND FUTURE WORK

In this paper, a novel approach to unroll deformed/post-mortem 3-D finger models in order to obtain 2-D rolled equivalent fingerprint images was proposed. With the intention to procure 2-D equivalent fingerprint, the algorithm included the following series of procedures: (i) masking and filtering, (ii) a non-parametric unrolling process preserving the Euclidean distance between points in the 3-D model. The robustness and feasibility of the method was tested by applying the algorithm on 3-D finger models of varying deformations. The results revealed that the 2-D equivalent unrolled deformed

fingerprints were visually similar to the 2-D equivalent unrolled normal fingerprint. However, significant spatial distortions were observed in models with very high deformations, which could lead to higher false rejection rates. The NIST fingerprint software was used to evaluate the quality of the unrolled fingerprint images, and these results help classify the unrolled outputs. In our ongoing research, we are studying the effects of pressure on fingers during rolled fingerprint acquisition. A method to simulate the pressure on finger models during 3-D unrolling is under current research. In the future, we look forward to implementing similar modeling schemes for other biometric modalities.

ACKNOWLEDGEMENTS

The research from this study was partially funded by the National Institute of Justice FY 2014 Research and Development in Forensic Science for Criminal Justice Purposes Grant Award # 2014-IJ-CX-K003, "Evaluation of the Use of A Non-Contact, 3D Scanner for Collecting Postmortem Fingerprints.". We would also like to thank Mike Troy, Marzena (Mary Ann) Mulawka, and Cole Wollak from FlashScan3D, LLC for their support in providing 3-D and 2-D input database and guidance.

REFERENCES

[1] A. K. Jain, Y. Chen, and M. Demirkus, "Pores and ridges: high-resolution fingerprint matching using level 3 features," Pattern Analysis and Machine Intelligence, IEEE Transactions on, 29(1), 15-27 (2007).
[2] D. Maltoni, and R. Cappelli, "Advances in fingerprint modeling," Image and Vision Computing, 27(3), 258-268 (2009).
[3] A. A. Khindre, and V. More, "An Approach to Touchless Fingerprint Recognition Using Matlab," International Journal of Emerging Trends & Technology in Computer Science (IJETTCS)-Volume, 3, 4 (2014).
[4] D. Maltoni, D. Maio, A. K. Jain *et al.*, [Handbook of fingerprint recognition] Springer Science & Business Media, (2009).
[5] A. K. Jain, J. Feng, and K. Nandakumar, "Fingerprint matching," Computer(2), 36-44 (2010).
[6] C. Tsikos, 'Capacitive fingerprint sensor', US4353056A, (1982)
[7] G. M. Fishbine, E. W. Laveen, J. M. Kaufman *et al.*, 'Optical fingerprinting system', 4,792,226., (1988)
[8] S. Bakhtiari, S. S. Agaian, and M. Jamshidi, "Local fingerprint image reconstruction based on gabor filtering." 840602-840602-11,(2012)
[9] S. Wang, and J. Hu, "Alignment-free cancelable fingerprint template design: A densely infinite-to-one mapping (DITOM) approach," Pattern Recognition, 45(12), 4129-4137 (2012).
[10] "Biometric Standards Requirements for US-VISIT", 2010}, http://www.dhs.gov/usvisit.
[11] Y. Song, C. Lee, and J. Kim, "A new scheme for touchless fingerprint recognition system." 524-527,(2004)
[12] W. Zhou, J. Hu, I. Petersen *et al.*, "Performance evaluation of 2D to 3D fingerprint recognition." 3, 1736-1741,(2013)
[13] Y. Wang, "Performance Analysis of 3-dimensional Fingerprint Scan System" University of Kentucky, (2008).
[14] S. Bakhtiari, "A Novel Method for Orientation Estimation in Highly Corrupted Fingerprint Images," International Journal of Intelligent Computing in Medical Sciences & Image Processing, 6(1), 45-63 (2014).
[15] F. Liu, and D. Zhang, "3D fingerprint reconstruction system using feature correspondences and prior estimated finger model," Pattern Recognition, 47(1), 178-193 (2014).
[16] S. J. Xie, J. Yang, S. Yoon *et al.*, "Fingerprint quality analysis and estimation for fingerprint matching," State of the art in Biometrics. Intech, Vienna. ISBN, 978-953 (2011).
[17] J.-J. Aguilar, F. Torres, and M. Lope, "Stereo vision for 3D measurement: accuracy analysis, calibration and industrial applications," Measurement, 18(4), 193-200 (1996).
[18] C. Lee, S. Lee, and J. Kim, "A study of touchless fingerprint recognition system" Springer, 358-365 (2006).
[19] G. Parziale, E. Diaz-Santana, and R. Hauke, "The surround imagertm: A multi-camera touchless device to acquire 3d rolled-equivalent fingerprints" Springer, 244-250 (2006).
[20] S. Shafaei, T. Inanc, and L. G. Hassebrook, "A new approach to unwrap a 3-d fingerprint to a 2-d rolled equivalent fingerprint." 1-5,(2009)
[21] Q. Zhao, A. Jain, and G. Abramovich, "3D to 2D fingerprints: Unrolling and distortion correction." 1-8,(2011)
[22] Y. Wang, L. G. Hassebrook, and D. L. Lau, "Data acquisition and processing of 3-D fingerprints," Information Forensics and Security, IEEE Transactions on, 5(4), 750-760 (2010).
[23] Y. Chen, G. Parziale, E. Diaz-Santana *et al.*, "3D touchless fingerprints: compatibility with legacy rolled images." 1-6,(2006)

[24] A. B. J. T. David Chek Ling Ngo, Jiankun Hu, “Biometric Security ”, 497/A5 (2015).
[25] G. Abramovich, K. Harding, S. Manickam *et al.*, "Mobile, contactless, single-shot, fingerprint capture system." 766708-766708-12,(2010)
[26] M. Mulawka, and L. Miller, [Postmortem Fingerprinting and Unidentified Human Remains] Routledge, (2014).
[27] B. T. Cutro Sr, “Recording Living and Postmortem Friction Ridge Exemplars,” The Fingerprint Sourcebook, 11 (2011).
[28] K. Rice, “Re-Hydration and Printing of Mummified Fingers,” Journal of Forensic Identification, 38(4), 152-156 (1988).
[29] A. Fatehpuria, D. L. Lau, and L. G. Hassebrook, "Acquiring a 2D rolled equivalent fingerprint image from a non-contact 3D finger scan." 62020C-62020C-8,(2006)
[30] C. B. Atkins, J. P. Allebach, and C. A. Bouman, “Halftone postprocessing for improved rendition of highlights and shadows,” Journal of Electronic Imaging, 9(2), 151-158 (2000).
[31] "FLASHSCAN3D LLC", http://www.flashscan3d.com/.
[32] D. L. Hassebrook, "MAT5 DATA FORMAT", http://www.engr.uky.edu/~lgh/soft/softmat5format.htm.
[33] Z. Wang, A. C. Bovik, H. R. Sheikh *et al.*, “Image quality assessment: from error visibility to structural similarity,” Image Processing, IEEE Transactions on, 13(4), 600-612 (2004).
[34] S. S. Agaian, K. Panetta, and A. M. Grigoryan, "A new measure of image enhancement." 19-22,(2000)
[35] K. Panetta, C. Gao, and S. Agaian, “No reference color image contrast and quality measures,” Consumer Electronics, IEEE Transactions on, 59(3), 643-651 (2013).
[36] K. Panetta, Y. Zhou, S. Agaian *et al.*, “Nonlinear unsharp masking for mammogram enhancement,” Information Technology in Biomedicine, IEEE Transactions on, 15(6), 918-928 (2011).
[37] C. I. Watson, M. D. Garris, E. Tabassi *et al.*, “User's guide to NIST biometric image software (NBIS),” (2007).